Exciting a Bound State in the Continuum through Multiphoton Scattering Plus Delayed Quantum Feedback

Giuseppe Calajó,[1,*] Yao-Lung L. Fang (方耀龍),[2,3,4] Harold U. Baranger,[2] and Francesco Ciccarello[2,5,6]

[1] *Vienna Center for Quantum Science and Technology, Atominstitut, TU Wien, Stadionallee 2, 1020 Vienna, Austria*
[2] *Department of Physics, Duke University, P.O. Box 90305, Durham, North Carolina 27708-0305, USA*
[3] *Computational Science Initiative, Brookhaven National Laboratory, Upton, NY 11973, USA*[†]
[4] *National Synchrotron Light Source II, Brookhaven National Laboratory, Upton, NY 11973, USA*[†]
[5] *Università degli Studi di Palermo, Dipartimento di Fisica e Chimica, via Archirafi 36, I-90123 Palermo, Italia*
[6] *NEST, Istituto Nanoscienze-CNR, Piazza S. Silvestro 12, 56127 Pisa, Italia*

(Dated: January 13, 2019)

Excitation of a bound state in the continuum (BIC) through scattering is problematic since it is by definition uncoupled. Here, we consider a type of dressed BIC and show that it can be excited in a nonlinear system through multi-photon scattering and delayed quantum feedback. The system is a semi-infinite waveguide with linear dispersion coupled to a qubit, in which a single-photon, dressed BIC is known to exist. We show that this BIC can be populated via multi-photon scattering in the non-Markovian regime, where the photon delay time (due to the qubit-mirror distance) is comparable with the qubit's decay. A similar process excites the BIC existing in an infinite waveguide coupled to two distant qubits, thus yielding stationary entanglement between the qubits. This shows, in particular, that single-photon trapping via multi-photon scattering can occur without band-edge effects or cavities, the essential resource being instead the *delayed* quantum feedback provided by a single mirror or the emitters themselves.

Introduction.—Waveguide Quantum ElectroDynamics (QED) is a growing area of quantum optics investigating the coherent interaction between quantum emitters and the one-dimensional (1D) field of a waveguide [1–3]. In such systems, a growing number of unique nonlinear and interference phenomena are being unveiled, the occurrence of which typically relies on the 1D nature of such setups. Among these is the formation of a class of bound states in the continuum (BIC), which are bound stationary states that arise *within* a continuum of unbound states [4]. Topical questions are how to form and prepare such states so as to enable potential applications such as quantum memory, which requires light trapping at the few-photon level, of interest for quantum information processing [5–7]. We show that addressing these questions involves studying delayed quantum dynamics in the presence of nonlinearity.

An interesting class of BICs occurs in waveguide QED in the form of dressed states featuring one or more emitters, usually qubits, dressed with a *single* photon that is strictly confined within a finite region [8–15]. The existence of such BICs relies on the *quantum feedback* provided by a mirror or the qubits themselves (since a qubit behaves as a perfect mirror under 1D single-photon resonant scattering [16, 17]). A natural way to populate these states is to excite the emitters and then let them decay: the system evolves towards the BIC with amplitude equal to the overlap between the BIC and the initial state. This results in incomplete decay of the emitter(s) and, in the case of two or more qubits, stationary entanglement [14, 15, 18–20]. As a hallmark, this approach for exciting BICs is most effective in the Markovian regime

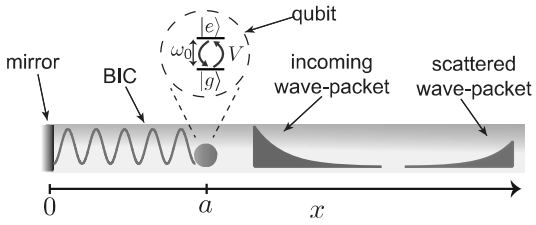

FIG. 1. One-qubit setup: a *semi-infinite* waveguide, whose end lies at $x = 0$ and acts as a perfect mirror, is coupled to a qubit at $x = a$. When a resonant standing wave can fit between the qubit and the mirror ($k_0 a = m\pi$), an incoming two-photon wavepacket is *not* necessarily fully scattered off the qubit: a fraction remains trapped in the form of a dressed single-photon BIC.

where the characteristic photonic *time delays*, denoted τ, are very short (e.g. the photon round-trip time between a qubit and mirror or between two qubits). Indeed, as the time delay grows, the qubit component of the BIC decreases in favor of the photonic component [11–13], making such decay-based schemes ineffective for large mirror-emitter or interemitter distances. This is a major limitation when entanglement creation is the goal [12].

In order to generate such dressed BICs in the non-Markovian regime of significant time delays, one needs initial states that overlap the BIC's photonic component, which in practice calls for *photon scattering*. A *single* photon scattered off the emitters cannot excite a BIC since the entire dynamics occurs in a sector of the Hilbert space orthogonal to the BIC. For *multi*-photon scattering,

however, this argument does not hold because of the intrinsic qubit nonlinearity. Indeed, the role of two-photon scattering has been recognized previously [21, 22] in the context of exciting normal bound states (i.e., outside the continuum) that occur in cavity arrays coupled to qubits [23–26].

We show that dressed BICs in waveguide-QED setups can be excited via multi-photon scattering in two paradigmatic setups: a qubit coupled to a semi-infinite waveguide (see Fig. 1) and a pair of distant qubits coupled to an infinite waveguide [see Fig. 5(a)]. A perfectly sinusoidal photon wavefunction and stationary excitation of the emitters represents a clear signature of single-photon trapping. This provides a solvable example of non-Markovian quantum dynamics in a nonlinear system, a scenario of interest in many areas of contemporary physics [27–33].

Model and BIC.—Consider first a qubit coupled to the 1D field of a semi-infinite waveguide [Fig. 1(a)] having a linear dispersion $\omega = v|k|$ (with v the photon group velocity and k the wavevector). The qubit's ground and excited states $|g\rangle$ and $|e\rangle$, respectively, are separated in energy by $\omega_0 = vk_0$ (we set $\hbar = 1$ throughout). The end of the waveguide at $x = 0$ is effectively a perfect mirror, while the qubit is placed at a distance a from the mirror. The Hamiltonian under the rotating wave approximation (RWA) reads [16, 34–37]

$$\hat{H} = \omega_0\,\hat{\sigma}^\dagger\hat{\sigma} - iv\int_0^\infty \mathrm{d}x\left[\hat{a}_R^\dagger(x)\frac{d}{dx}\hat{a}_R(x) - \hat{a}_L^\dagger(x)\frac{d}{dx}\hat{a}_L(x)\right] + V\int_0^\infty \mathrm{d}x\left[\left(\hat{a}_L^\dagger(x)+\hat{a}_R^\dagger(x)\right)\hat{\sigma} + \mathrm{H.c.}\right]\delta(x-a)\,, \tag{1}$$

with $\hat{\sigma} = |g\rangle\langle e|$, $\hat{a}_{R(L)}(x)$ the bosonic field operator annihilating a right-going (left-going) photon at position x, and V the atom-photon coupling. Due to the RWA, the total number of excitations $\hat{N} = \hat{\sigma}^\dagger\hat{\sigma} + \sum_{\eta=R,L}\int \mathrm{d}x\,\hat{a}_\eta^\dagger(x)\hat{a}_\eta(x)$ is conserved.

In the single-excitation subspace ($N = 1$), the spectrum of (1) comprises an infinite continuum of unbound dressed states $\{|\phi_k\rangle\}$ with energy $\omega_k = v|k|$ [12, 16, 34–37], each a scattering eigenstate in which an incoming photon is completely reflected. Notably, a further stationary state $|\phi_b\rangle$ exists when the condition $k_0 a = m\pi$ (with $m = 0, 1, \cdots$) is met. This BIC has the same energy $\omega_b = \omega_0$ as the qubit and is given by [11, 38]

$$|\phi_b\rangle = \varepsilon_b\left[\hat{\sigma}^\dagger \pm i\sqrt{\tfrac{\Gamma}{2v}}\int_0^a \mathrm{d}x\left(e^{ik_0x}\hat{a}_R^\dagger(x) - e^{-ik_0x}\hat{a}_L^\dagger(x)\right)\right]|g\rangle|0\rangle \tag{2}$$

with $\Gamma = 2V^2/v$ the qubit's decay rate (without mirror). The qubit's excited-state population (referred to simply as "population" henceforth) is given by

$$|\varepsilon_b|^2 = \frac{1}{1+\frac{1}{2}\Gamma\tau}\,, \tag{3}$$

where $\tau = 2a/v$ is the *delay time*. Eqs. (2) and (3) fully specify the BIC. The photonic wavefunction has shape [we set $|x\rangle = \hat{a}^\dagger(x)|0\rangle$ with $\hat{a}^\dagger(x) = \left(\hat{a}_R^\dagger(x) + \hat{a}_L^\dagger(x)\right)$]

$$\langle x|\phi_b\rangle \propto \sin(k_0 x) \quad \text{for } 0 \le x \le a\,, \tag{4}$$

while it vanishes at $x \notin [0, a]$: the BIC is formed strictly between the qubit and the mirror, where the field profile is a pure sinusoid. When the BIC exists (i.e., for $k_0 a = m\pi$) the qubit does not fully decay in vacuum [11, 39, 40]: since the overlap of the initial state $|e, 0\rangle$ with the BIC is ε_b, $|\varepsilon_b|^2$ is also the probability of generating the BIC via vacuum decay. This probability decreases monotonically with delay time [Eq. (3)], showing that vacuum decay is most effective when $\Gamma\tau$ is small.

BIC generation scheme.—Bound state (2) cannot be generated, however, via single-photon scattering, which involves only the unbound states $\{|\phi_k\rangle\}$ that are all orthogonal to $|\phi_b\rangle$: during a transient time the photon may be absorbed by the qubit, but it is eventually fully released. We thus send a *two-photon* wavepacket such that the initial joint state is $|\Psi(0)\rangle = A\iint_0^\infty \mathrm{d}x\mathrm{d}y\,\left[\varphi_1^L(x)\varphi_2^L(y) + 1 \leftrightarrow 2\right]\hat{a}_L^\dagger(x)\hat{a}_L^\dagger(y)|g\rangle|0\rangle$, where A is for normalization, $\varphi_i^L(x)$ is the wavefunction of a single left-propagating photon, and the qubit is not excited. The ensuing dynamics in the two-excitation sector ($N = 2$) is given by

$$|\Psi(t)\rangle = \left[\sum_{\eta=R,L}\int_0^\infty \mathrm{d}x\,\psi_\eta(x,t)\hat{a}_\eta^\dagger(x)\hat{\sigma}^\dagger + \sum_{\eta,\eta'=R,L}\tfrac{1}{\sqrt{2}}\iint_0^\infty \mathrm{d}x\mathrm{d}y\,\chi_{\eta\eta'}(x,y,t)\hat{a}_\eta^\dagger(x)\hat{a}_{\eta'}^\dagger(y)\right]|g\rangle|0\rangle, \tag{5}$$

where $\chi_{\eta\eta'}(x, y, t)$ is the wavefunction of the two-photon component while $\psi_\eta(x, t)$ is the amplitude that the qubit is excited and a right-(left-) propagating photon is found at position x. We define

$$P_\mathrm{e}(t) \equiv \sum_{\eta=R,L}\int_0^\infty \mathrm{d}x\,|\psi_\eta(x,t)|^2,$$
$$P_\mathrm{ph}(t) \equiv 2\sum_{\eta,\eta'=R,L}\int_0^a \mathrm{d}x\int_a^\infty \mathrm{d}y\,|\chi_{\eta\eta'}(x,y,t)|^2 \tag{6}$$

as, respectively, the qubit population and the probability that one photon lies in region $[0, a]$ and one in (a, ∞).

We first consider for simplicity a two-photon exponential wavepacket (sketched in Fig. 1): $\varphi_{1,2}^L(x) = e^{-\Delta k|x-a| - ik_0(x-a)}\theta(x-a)$ where $v\Delta k$ is the bandwidth, the carrier wavevector k_0 is resonant with the qubit, and the wavefront reaches the qubit at $t = 0$. In Fig. 2, we plot results for the dynamics described by (1) obtained numerically (for details see [41]). As the wavepacket impinges on the qubit, its population P_e [Fig. 2(a)] exhibits

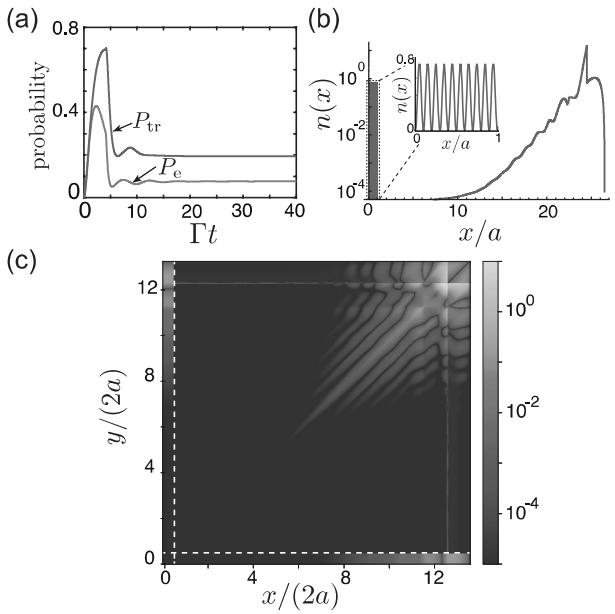

FIG. 2. BIC generation via two-photon scattering. (a) Qubit population $P_{\rm e}$ and trapping probability $P_{\rm tr}$ as a function of time in units of Γ^{-1}. (b) Spatial profile of the field intensity $n(x)$ at the end of scattering. The inset highlights the sinusoidal wavefunction in the range $0 \le x \le a$. (c) Two-photon probability density function $\sum_{\eta,\eta'=R,L} |\chi_{\eta\eta'}(x,y)|^2$ after scattering is complete ($t = t_f$). The white dashed lines x=a and y=a mark the qubit position. [Panels (b) and (c) are plotted on a log scale and with t_f=$80/\Gamma$. We considered a two-photon exponential wavepacket with $\Gamma\tau = \pi$, $k_0 a = 10\pi$ and $\Delta k = \Gamma/2v$.]

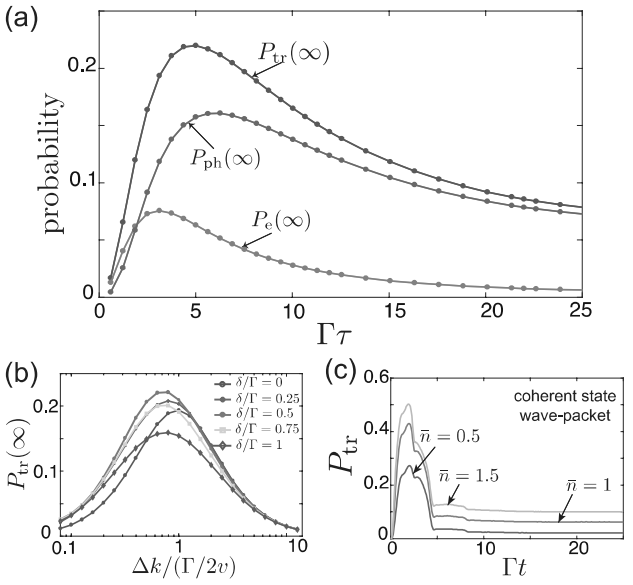

FIG. 3. (a) Asymptotic values of $P_{\rm e}$, $P_{\rm ph}$, and $P_{\rm tr}$ as a function of the rescaled time delay $\Gamma\tau$ for $\delta = 0$. At each point, Δk is set so as to maximize $P_{\rm tr}$. Here we used the optimized Δk shown in [41]. (b) Asymptotic value of $P_{\rm tr}(\infty) = P_{\rm BIC}$ against the wavepacket bandwidth for $\Gamma\tau = \pi$, $k_0 a = 10\pi$ and different values of detuning δ, where we assumed that one photon has carrier wavevector $k_1 = k_0 + \delta/v$ and the other has $k_2 = k_0 - \delta/v$. (c) $P_{\rm tr}$ versus time for coherent-state wavepackets with the same shape. For computational reasons, only contributions up to three-photon Fock states are retained. The parameters are the same as in Fig. 2.

a rise followed by a drop (photon absorption then re-emission) eventually converging to a small — yet *finite* — steady value. This shows that part of the excitation absorbed from the wavepacket is never released back.

The photon field in the same process is shown in Figs. 2(b) and 2(c) displaying, respectively, the field intensity $n(x) = \langle\Psi(t_f)|\hat{a}^\dagger(x)\hat{a}(x)|\Psi(t_f)\rangle$ and the total two-photon probability density $\sum_{\eta,\eta'=R,L} |\chi_{\eta\eta'}(x,y,t_f)|^2$ at a time t_f after the scattering process is complete. The wavepacket is not entirely reflected back: a significant fraction remains trapped between the mirror and qubit, forming a perfectly sinusoidal wave with wavevector k_0 [Fig. 2(b)]. Remarkably, this stationary wave is of single-photon nature. Indeed, Fig. 2(c) shows that either both photons are reflected (top right corner) or one is scattered and the other remains trapped in the mirror-qubit interspace (top left and bottom right). Note that the probability that both photons are trapped (bottom left) is zero.

These outcomes, in light of the features of the BIC (2), suggest that, after scattering, the joint state has the form

$$|\Psi(t_f)\rangle = \int_a^\infty \mathrm{d}x\, \xi_R(x,t_f)\hat{a}_R^\dagger(x)|\phi_b\rangle + \iint_a^\infty \mathrm{d}x\mathrm{d}y\, \beta_{RR}(x,y,t_f)\, \hat{a}_R^\dagger(x)\hat{a}_R^\dagger(y)|g,0\rangle\,, \tag{7}$$

where in the first line a single photon has left the BIC region, while the last line describes two outgoing photons. Let $P_{\rm tr} = P_{\rm e} + P_{\rm ph}$ be the probability that either the qubit is excited or a photon is trapped between the mirror and qubit. It then follows from (7) [41] that the asymptotic values of $P_{\rm tr}$ and $P_{\rm e}$ fulfill

$$P_{\rm tr}(\infty) = \int_a^\infty \mathrm{d}x\, |\xi_R(x,\infty)|^2 = \left(1 + \tfrac{1}{2}\Gamma\tau\right) P_{\rm e}(\infty), \tag{8}$$

which is naturally interpreted as the probability of generating the BIC, $P_{\rm BIC} \equiv P_{\rm tr}(\infty)$. The time dependence of $P_{\rm tr}$ shown in Fig. 2(a) demonstrates that it reaches a finite steady value satisfying (8), confirming Eq. (7) and thus, the generation of the BIC. The identity (8) was checked in all of the numerical results presented.

Dependence on time delay.—A substantial delay time is essential for exciting the BIC. The parameter set in

Fig. 2, for instance, corresponds to $\Gamma\tau \simeq 3.14$. To highlight this dependence, we report in Fig. 3(a) the steady state values of $P_{\rm e}$, $P_{\rm ph}$, and $P_{\rm tr}$, optimized with respect to Δk, as functions of $\Gamma\tau$. Both photon trapping and stationary qubit excitation are negligible in the Markovian regime $\Gamma\tau \ll 1$, in sharp contrast to vacuum-decay schemes for which this is instead the optimal regime. A delay time $\Gamma\tau \gtrsim 1$ is required to make our BIC generation scheme effective; indeed, each of the three probabilities reaches a maximum at a delay of order $\Gamma\tau \sim 1$. Remarkably, $P_{\rm e}$ becomes negligible compared to $P_{\rm ph}$ for $\Gamma\tau \gtrsim 10$, showing that the photon component is dominant at large delays as expected from Eqs. (2) and (3): In this regime, we thus get almost *pure* single-photon trapping

Dependence on bandwidth and detuning.—The efficiency of BIC generation depends on the width, Δk, of the injected wavepacket. In Fig. 3(b) the optimal value is close to $\Gamma/2v$. Thus, photon absorption is maximum when the wavepacket width is of order the qubit decay rate, in agreement with general expectations [42–44]. The optimal Δk as a function of delay time is given in the supplemental material [41]; for large $\Gamma\tau$, the optimal value saturates near $0.2\Gamma/v$.

Non-resonant photons can also be used to generate the BIC: results for a wavepacket of two photons detuned oppositely in energy are shown in Fig. 3(b). The optimal wavepacket width changes but remains of order Γ. As the detuning increases, the maximum $P_{\rm BIC}$ initially rises and then decays; note that the optimal detuning is $\delta \approx \Gamma/2$. At this value the nonlinear scattering flux was shown to peak [45, 46], confirming that the intrinsic *nonlinearity* of the emitters is key to generating the BIC [41].

Coherent-state wavepacket.—It is natural to wonder whether, instead of a two-photon pulse, the BIC can be excited using a coherent-state wavepacket, which is easier to generate experimentally. In Fig. 3(c) we consider the same setup, parameters, and wavepacket shape $\varphi(x)$ as in Fig. 2 but for a low-power coherent-state pulse [36] $|\alpha\rangle = e^{-|\alpha|^2}\sum_{n=0}^{\infty}(\alpha^n/n!)\left(\int {\rm d}x\varphi(x)\hat{a}_L^\dagger(x)\right)^n|g,0\rangle$ with the average photon number given by $\bar{n} = |\alpha|^2$. For $\bar{n} = 1.5$, $P_{\rm tr}(\infty)$ is comparable to the one obtained with the two-photon pulse, demonstrating the effectiveness of using coherent states.

Increasing the BIC generation probability.—We find that the trapping probability depends sensitively on the shape of the incoming wavepacket. While we have mostly used (Figs. 2, 3, 5) the exponential pulse that is standard in the literature [44, 47], Fig. 4 shows how engineering the wavepacket shape strongly enhances $P_{\rm BIC}$ [48]. We set here $\Gamma\tau = 5$, which roughly corresponds to the maximum of $P_{\rm tr}(\infty) = P_{\rm BIC}$ in Fig. 3(a). The engineered incoming two-photon wavepacket in Fig. 4(a) (for methods see [41]) yields $P_{\rm BIC} \simeq 80\%$, a value about four times larger.

Two-qubit BIC.— A BIC very similar to the one addressed above occurs in an infinite waveguide (no mirror) coupled to a pair of identical qubits [8, 10, 12–15]. With the qubits placed at $x_1 = -a/2$ and $x_2 = a/2$ and for $k_0 a = m\pi$ [Fig. 5(a)], there exists a BIC given by

$$|\varphi_b\rangle = \varepsilon_b\left[\hat{\sigma}_\pm^\dagger - i\sqrt{\tfrac{\Gamma}{4v}}\int_{-a/2}^{a/2}{\rm d}x\left(e^{ik_0(x+a/2)}\hat{a}_R^\dagger(x) - e^{-ik_0(x+a/2)}\hat{a}_L^\dagger(x)\right)\right]|g_1,g_2\rangle|0\rangle, \tag{9}$$

where now $|\varepsilon_b|^2 = 1/(1+\Gamma\tau/4)$, $\hat{\sigma}_\pm = (\hat{\sigma}_1 \pm \hat{\sigma}_2)/\sqrt{2}$, and plus (minus) is used if m is odd (even). By tracing out the photonic field, Eq. (9) clearly entails *entanglement* between the qubits. (In the familiar limit $\Gamma\tau \ll 1$, for instance, the entangled state is $\hat{\sigma}_\pm^\dagger|g_1,g_2\rangle|0\rangle$, namely the sub- or super-radiant, maximally entangled state [18–20, 37, 49–51].) Thus, in the two-qubit setup of Fig. 5(a), our scattering-based approach to exciting the BIC can in particular generate entanglement.

This expectation is confirmed in Fig. 5(b), for which the same injected exponential wavepacket was used as in Fig. 2. In addition to the probability to excite at least one qubit $P_{\rm e}$ and the probability to generate a BIC (9), we plot the amount of entanglement between the qubits, as measured by the concurrence C [52]. As for one qubit, the two-qubit BIC population reaches a steady value after scattering, resulting in an excitation stored in the qubits and hence stationary entanglement. Note the typical [53] "sudden birth" of the entanglement.

Conclusions.—We have shown that dressed BICs occurring in waveguide-QED setups can be generated via multi-photon scattering. This enables single-photon capture and, for multiple emitters, production of stationary entanglement. These BICs differ significantly from purely excitonic subradiant states, as well as from BICs located entirely within the side-coupled quantum system, in that they involve the field of the waveguide itself.

For our method, it is critical to have *nonlinear* emitters such as qubits; replacing them by bosonic modes, for example, will invalidate the whole scheme [41].

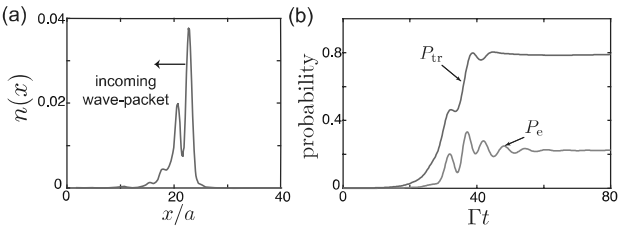

FIG. 4. BIC generation scheme for the one-qubit setup using a structured-shape two-photon wavepacket (see [41]). (a) Photon density profile of the incoming wavepacket. (b) $P_{\rm BIC}$ and $P_{\rm e}$ versus time. For this plot we fixed the distance to $k_0 a = 20\pi$ and the time delay to $\Gamma\tau = 5$ to maximize the photon trapping probability [see Fig. 3(b)].

While preparing this Letter we became aware of a related scheme by Cotrufo and Alù [48]. There however the BIC arises from a single system, comprised of a qubit and two cavities to provide feedback, side-coupled to an infinite waveguide. Here, instead, no cavities are present and the necessary quantum feedback is provided by a mirror [cf. Fig. 1] or the emitters themselves [cf. Fig. 5(a)]. Remarkably, in order to generate the BIC, this feedback needs to be *delayed* [cf. Fig. 3(a)].

Investigating the non-Markovian effects of non-negligible delays is a new frontier of quantum optics [11, 13, 30–33, 37, 39, 44, 51, 54–69]. Here we have taken advantage of such delays, demonstrating that their role can be constructive [63, 68]. In particular, within the range considered, as shown in Fig. 3(a), long delays ($\Gamma\tau \gtrsim 20$) enable almost pure single-photon trapping (instead of hybrid atom-photon excitation). Remarkably, adding qubit losses, denoted by γ_a, makes the trapped photon decay slowly at the rate $\gamma_a|\varepsilon_b|^2$ [41], suggesting that our scheme is more robust against emitter loss for larger delay τ.

Targets of ongoing investigation include exploring the regime of very long delays (beyond $\Gamma\tau \simeq 25$ in Fig. 3(a) allowed by our current computational capabilities [41]) and deriving a systematic criterion to increase the generation probability by wavepacket engineering (possibly by exploiting time reversal symmetry [42, 48]). We expect this line of research will become important to, for example, long-distance communication over quantum networks.

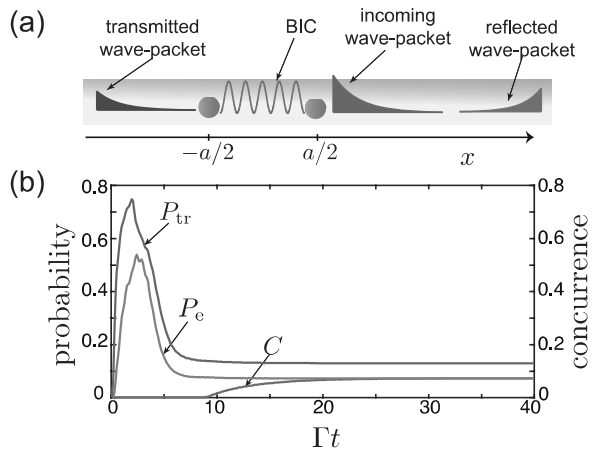

FIG. 5. (a) Two-qubit setup: an *infinite* waveguide (no mirror) is coupled to a pair of qubits. (b) Probability to excite at least one qubit $P_{\rm e}$, trapping probability $P_{\rm tr}$, and qubit-qubit concurrence C versus time in a two-photon scattering process (see [41] for definition of $P_{\rm e}$, $P_{\rm tr}$ and C). The wavepacket and parameters are the same as in Fig. 2. The scheme generates a dressed BIC in a way analogous to the one-qubit setup in Fig. 1, yielding however stationary entanglement between the qubits.

We thank Peter Rabl, Shanhui Fan, and Tommaso Tufarelli for useful discussions. We acknowledge support from the U.S. DOE Office of Science Division of Materials Sciences and Engineering under Grant No. de-sc0005237 and the Fulbright Research Scholar Program. The work at BNL was supported in part by BNL LDRD projects No. 17-029 and No. 19-002, and New York State Urban Development Corporation, d/b/a Empire State Development, under contract No. AA289. G. C. acknowledges support from the Austrian Science Fund (FWF) through SFB FOQUS F40, DK CoQuS W 1210, and the START grant Y 591-N16. Part of the computation was completed using resources of the Center for Functional Nanomaterials, which is a U.S. DOE Office of Science Facility, and the Scientific Data and Computing Center, a component of the Computational Science Initiative, at Brookhaven National Laboratory under Contract No. de-sc0012704.

* Present address: ICFO-Institut de Ciencies Fotoniques, 08860 Castelldefels (Barcelona), Spain. Contact email giuseppe.calajo@icfo.eu.
† Present address

[1] Z. Liao, X. Zeng, H. Nha, and M. S. Zubairy, "Photon transport in a one-dimensional nanophotonic waveguide QED system," Phys. Scr. **91**, 063004 (2016).
[2] D. Roy, C. M. Wilson, and O. Firstenberg, "Colloquium: Strongly interacting photons in one-dimensional continuum," Rev. Mod. Phys. **89**, 021001 (2017).
[3] X. Gu, A. F. Kockum, A. Miranowicz, Y. X. Liu, and F. Nori, "Microwave photonics with superconducting quantum circuits," Phys. Rep. **718**, 1–102 (2017).
[4] C. W. Hsu, B. Zhen, A. D. Stone, J. D. Joannopoulos, and M. Soljačić, "Bound states in the continuum," Nat. Rev. Mater. **1**, 16048 (2016).
[5] H. J. Kimble, "The quantum internet," Nature **453**, 1023 (2008).
[6] A. I. Lvovsky, B. C. Sanders, and W. Tittel, "Optical quantum memory," Nat. Photonics **3**, 706 (2009).
[7] E. Saglamyurek, T. Hrushevskyi, A. Rastogi, K. Heshami, and L. J. LeBlanc, "Coherent storage and manipulation of broadband photons via dynamically controlled Autler–Townes splitting," Nat. Photonics (2018).
[8] G. Ordonez, K. Na, and S. Kim, "Bound states in the continuum in quantum-dot pairs," Phys. Rev. A **73**, 022113 (2006).
[9] S. Longhi, "Bound states in the continuum in a single-level Fano-Anderson model," Eur. Phys. J. B **57**, 45–51 (2007).
[10] S. Tanaka, S. Garmon, G. Ordonez, and T. Petrosky, "Electron trapping in a one-dimensional semiconductor quantum wire with multiple impurities," Phys. Rev. B **76**, 153308 (2007).
[11] T. Tufarelli, F. Ciccarello, and M. S. Kim, "Dynamics of spontaneous emission in a single-end photonic waveguide," Phys. Rev. A **87**, 013820 (2013).
[12] C. Gonzalez-Ballestero, F. J. Garcia-Vidal, and E. Moreno, "Non-Markovian effects in waveguide-mediated entanglement," New J. Phys. **15**, 073015

(2013).
[13] E. S. Redchenko and V. I. Yudson, "Decay of metastable excited states of two qubits in a waveguide," Phys. Rev. A **90**, 063829 (2014).
[14] P. Facchi, M. S. Kim, S. Pascazio, F. V. Pepe, D. Pomarico, and T. Tufarelli, "Bound states and entanglement generation in waveguide quantum electrodynamics," Phys. Rev. A **94**, 043839 (2016).
[15] P. Facchi, S. Pascazio, F. V. Pepe, and K. Yuasa, "Long-lived entanglement of two multilevel atoms in a waveguide," J. Phys. Commun. **2**, 035006 (2018).
[16] J. T. Shen and S. Fan, "Coherent single photon transport in a one-dimensional waveguide coupled with superconducting quantum bits," Phys. Rev. Lett. **95**, 213001 (2005).
[17] D. E. Chang, A. S. Sørensen, E. A. Demler, and M. D. Lukin, "A single-photon transistor using nanoscale surface plasmons," Nature Phys. **3**, 807–812 (2007).
[18] A. González-Tudela, D. Martin-Cano, E. Moreno, L. Martín-Moreno, and F. Tejedor, C./García-Vidal, "Entanglement of two qubits mediated by one-dimensional plasmonic waveguides," Phys. Rev. Lett. **106**, 020501 (2011).
[19] A. González-Tudela and D. Porras, "Mesoscopic entanglement induced by spontaneous emission in solid-state quantum optics," Phys. Rev. Lett. **110**, 080502 (2013).
[20] D. E. Chang, L. Jiang, A. V. Gorshkov, and H. J. Kimble, "Cavity QED with atomic mirrors," New J. Phys. **14**, 063003 (2012).
[21] P. Longo, P. Schmitteckert, and K. Busch, "Few-photon transport in low-dimensional systems: Interaction-induced radiation trapping," Phys. Rev. Lett. **104**, 023602 (2010).
[22] P. Longo, P. Schmitteckert, and K. Busch, "Few-photon transport in low-dimensional systems," Phys. Rev. A **83**, 063828 (2011).
[23] F. Lombardo, F. Ciccarello, and G. M. Palma, "Photon localization versus population trapping in a coupled-cavity array," Phys. Rev. A **89**, 053826 (2014).
[24] G. Calajó, F. Ciccarello, D. E. Chang, and P. Rabl, "Atom-field dressed states in slow-light waveguide QED," Phys. Rev. A **93**, 033833 (2016).
[25] T. Shi, Y.-H. Wu, A. González-Tudela, and J. I. Cirac, "Bound states in boson impurity models," Phys. Rev. X **6**, 021027 (2016).
[26] Ş. E. Kocabaş, "Effects of modal dispersion on few-photon–qubit scattering in one-dimensional waveguides," Phys. Rev. A **93**, 033829 (2016).
[27] P. K. Shukla and B. Eliasson, "Colloquium: Nonlinear collective interactions in quantum plasmas with degenerate electron fluids," Rev. Mod. Phys. **83**, 885–906 (2011).
[28] I. García-Mata, C. Pineda, and D. A. Wisniacki, "Quantum non-Markovian behavior at the chaos border," J. Phys. A **47**, 115301 (2014).
[29] B. Swingle, "Unscrambling the physics of out-of-time-order correlators," Nat. Phys. **14**, 988–990 (2018).
[30] H. Ritsch, P. Domokos, F. Brennecke, and T. Esslinger, "Cold atoms in cavity-generated dynamical optical potentials," Rev. Mod. Phys. **85**, 553–601 (2013).
[31] M. Aspelmeyer, T. J. Kippenberg, and F. Marquardt, "Cavity optomechanics," Rev. Mod. Phys. **86**, 1391–1452 (2014).
[32] Z. Wang and A. H. Safavi-Naeini, "Enhancing a slow and weak optomechanical nonlinearity with delayed quantum feedback," Nat. Commun. **8**, 15886 (2017).
[33] M. Rossi, N. Kralj, S. Zippilli, R. Natali, A. Borrielli, G. Pandraud, E. Serra, G. Di Giuseppe, and D. Vitali, "Normal-mode splitting in a weakly coupled optomechanical system," Phys. Rev. Lett. **120**, 073601 (2018).
[34] J.-T. Shen and S. Fan, "Strongly correlated multiparticle transport in one dimension through a quantum impurity," Phys. Rev. A **76**, 062709 (2007).
[35] J.-T. Shen and S. Fan, "Theory of single-photon transport in a single-mode waveguide," Phys. Rev. A **79**, 023837 (2009).
[36] H. Zheng, D. J. Gauthier, and H. U. Baranger, "Waveguide QED: Many-body bound-state effects in coherent and Fock-state scattering from a two-level system," Phys. Rev. A **82**, 063816 (2010).
[37] H. Zheng and H. U. Baranger, "Persistent quantum beats and long-distance entanglement from waveguide-mediated interactions," Phys. Rev. Lett. **110**, 113601 (2013).
[38] Here the plus sign occurs for m even, while the minus sign is for m odd.
[39] T. Tufarelli, M. S. Kim, and F. Ciccarello, "Non-Markovianity of a quantum emitter in front of a mirror," Phys. Rev. A **90**, 012113 (2014).
[40] I.-C. Hoi, A. F. Kockum, L. Tornberg, A. Pourkabirian, G. Johansson, P. Delsing, and C. M. Wilson, "Probing the quantum vacuum with an artificial atom in front of a mirror," Nat. Phys. **11**, 1045–1049 (2015).
[41] See Supplementary Material at [URL] for computational methods used in this work (see also Ref. [70]), derivation of Eq. (8), optimal Δk used in Fig. 3(a), explanation of the method used to increase BIC generation probability in Fig. 4, additional notes on the two-qubit BIC, impact of nonzero loss to photon trapping, and the importance of having nonlinear emitters.
[42] M. Stobińska, G. Alber, and G. Leuchs, "Perfect excitation of a matter qubit by a single photon in free space," Eur.ophys. Lett. **86**, 14007 (2009).
[43] B. Q. Baragiola, R. L. Cook, A. M. Brańczyk, and J. Combes, "N-photon wave packets interacting with an arbitrary quantum system," Phys. Rev. A **86**, 013811 (2012).
[44] Y.-L. L. Fang, F. Ciccarello, and H. U. Baranger, "Non-Markovian dynamics of a qubit due to single-photon scattering in a waveguide," New J. Phys. **20**, 043035 (2018).
[45] Y.-L. L. Fang and H. Baranger, "Photon correlations generated by inelastic scattering in a one-dimensional waveguide coupled to three-level systems," Physica **78E**, 92–99 (2016).
[46] Y.-L. L. Fang and H. U. Baranger, "Multiple emitters in a waveguide: Nonreciprocity and correlated photons at perfect elastic transmission," Phys. Rev. A **96**, 013842 (2017).
[47] E. Rephaeli and S. Fan, "Stimulated emission from a single excited atom in a waveguide," Phys. Rev. Lett. **108**, 143602 (2012).
[48] M. Cotrufo and A. Alù, "Single-photon embedded eigenstates in coupled cavity-atom systems," (2018), arXiv:1805.03287.
[49] K. Lalumière, B. C. Sanders, A. F. van Loo, A. Fedorov, A. Wallraff, and A. Blais, "Input-output theory for waveguide QED with an ensemble of inhomogeneous atoms," Phys. Rev. A **88**, 043806 (2013).
[50] A. F. van Loo, A. Fedorov, K. Lalumière, B. C. Sanders,

A. Blais, and A. Wallraff, "Photon-Mediated Interactions Between Distant Artificial Atoms," Science **342**, 1494–1496 (2013).
[51] Y.-L. L. Fang and H. U. Baranger, "Waveguide QED: Power spectra and correlations of two photons scattered off multiple distant qubits and a mirror," Phys. Rev. A **91**, 053845 (2015), *ibid.* **96**, 059904(E) (2017).
[52] W. K. Wootters, "Entanglement of formation of an arbitrary state of two qubits," Phys. Rev. Lett. **80**, 2245–2248 (1998).
[53] Z. Ficek and R. Tanaś, "Delayed sudden birth of entanglement," Phys. Rev. A **77**, 054301 (2008).
[54] U. Dorner and P. Zoller, "Laser-driven atoms in half-cavities," Phys. Rev. A **66**, 023816 (2002).
[55] A. Carmele, J. Kabuss, F. Schulze, S. Reitzenstein, and A. Knorr, "Single Photon Delayed Feedback: A Way to Stabilize Intrinsic Quantum Cavity Electrodynamics," Phys. Rev. Lett. **110**, 013601 (2013).
[56] M. Laakso and M. Pletyukhov, "Scattering of two photons from two distant qubits: Exact solution," Phys. Rev. Lett. **113**, 183601 (2014).
[57] A. L. Grimsmo, "Time-Delayed Quantum Feedback Control," Phys. Rev. Lett. **115**, 060402 (2015).
[58] H. Pichler and P. Zoller, "Photonic Circuits with Time Delays and Quantum Feedback," Phys. Rev. Lett. **116**, 093601 (2016).
[59] T. Ramos, B. Vermersch, P. Hauke, H. Pichler, and P. Zoller, "Non-Markovian dynamics in chiral quantum networks with spins and photons," Phys. Rev. A **93**, 062104 (2016).
[60] G. Tabak and H. Mabuchi, "Trapped modes in linear quantum stochastic networks with delays," EPJ Quantum Technol. **3**, 3 (2016).
[61] S. J. Whalen, A. L. Grimsmo, and H. J. Carmichael, "Open quantum systems with delayed coherent feedback," Quantum Science and Technology **2**, 044008 (2017).
[62] P.-O. Guimond, M. Pletyukhov, H. Pichler, and P. Zoller, "Delayed coherent quantum feedback from a scattering theory and a matrix product state perspective," Quantum Sci. Technol. **2**, 044012 (2017).
[63] H. Pichler, S. Choi, P. Zoller, and M. D. Lukin, "Universal photonic quantum computation via time-delayed feedback," Proc. Natl. Acad. Sci. **114**, 11362–11367 (2017).
[64] L. Guo, A. Grimsmo, A. F. Kockum, M. Pletyukhov, and G. Johansson, "Giant acoustic atom: A single quantum system with a deterministic time delay," Phys. Rev. A **95**, 053821 (2017).
[65] H. Chalabi and E. Waks, "Interaction of photons with a coupled atom-cavity system through a bidirectional time-delayed feedback," Phys. Rev. A **98**, 063832 (2018).
[66] G. Tabak, R. Hamerly, and H. Mabuchi, "Factorization of linear quantum systems with delayed feedback," (2018), arXiv:1803.01539.
[67] C.-Y. Chang, L. Lanco, P. Senellart, and D. S. Citrin, "Quantum stabilization of a single-photon emitter in a coupled microcavity–half-cavity system," (2018), arXiv:1804.06734.
[68] G. Torre and F. Illuminati, "Non-Markovianity-assisted optimal continuous variable quantum teleportation," (2018), arXiv:1805.03617.
[69] G. Andersson, B. Suri, L. Guo, T. Aref, and P. Delsing, "Nonexponential decay of a giant artificial atom," (2018), arXiv:1812.01302.
[70] Y.-L. L. Fang, "FDTD: Solving 1+1D delay PDE in parallel," Comput. Phys. Commun. **235**, 422 – 432 (2019).

Supplementary Material for "Exciting a Bound State in the Continuum through Multiphoton Scattering Plus Delayed Quantum Feedback"

Giuseppe Calajó,[1] Yao-Lung L. Fang (方耀龍),[2,3,4] Harold U. Baranger,[2] and Francesco Ciccarello[2,5,6]

[1] *Vienna Center for Quantum Science and Technology, Atominstitut, TU Wien, Stadionallee 2, 1020 Vienna, Austria**

[2] *Department of Physics, Duke University, P.O. Box 90305, Durham, North Carolina 27708-0305, USA*

[3] *Computational Science Initiative, Brookhaven National Laboratory, Upton, NY 11973, USA†*

[4] *National Synchrotron Light Source II, Brookhaven National Laboratory, Upton, NY 11973, USA†*

[5] *Università degli Studi di Palermo, Dipartimento di Fisica e Chimica, via Archirafi 36, I-90123 Palermo, Italia*

[6] *NEST, Istituto Nanoscienze-CNR, Piazza S. Silvestro 12, 56127 Pisa, Italia*

(Dated: January 13, 2019)

CONTENTS

COMPUTATIONAL METHODS

In order to solve for various wavefunctions in the waveguide-QED setups that we consider, we have taken two different routes: treating the 1D field as a continuum or discretizing it as an effective coupled-cavity array (CCA) and working in the middle of the band, where band-edge effects are minimized and the dispersion is close to linear. In the main text, results shown in Figs. 2 and 3(a)-(b) were obtained through the continuum approach, while the discrete approach was employed for producing Figs. 3(c), 4 and 5.

Continuum approach

For the continuum case, we follow the approach reported in Ref. [S1]: Starting from the Schrödinger equation, by unfolding the half space and tracing out the two-photon part, we arrive at a (1+1)-dimensional *delay* partial differential equation for the wavefunction $\psi(x,t)$ [joint amplitude for qubit and one photon at position x, c.f. Eq. (5) of the main text], which we solve using a tailored finite-difference time-domain (FDTD) code that has multithreading support for reducing the computation time considerably [S2].[1] The two-photon wavefunction can be constructed

[1] This FDTD code is open-sourced at `https://github.com/leofang/FDTD` and also available in Ref. [S2].

straightforwardly once ψ is solved [S1, S2]. Our FDTD code provides the numerically exact solution to the dynamics in the two-excitation sector.

For solving the two-photon scattering problem of interest, we send in a two-photon exponential wavepacket with the qubit initially unexcited (set `init_cond=3` in the code). In the region $x < -a$, the exact solution to ψ is given by

$$\psi(x < -a, t) = A\left[\varphi_1(x - vt)e_0^{(2)}(t) + \varphi_2(x - vt)e_0^{(1)}(t)\right], \tag{S1}$$

where $e_0^{(i)}(t)$ is the qubit wavefunction in the one-excitation sector, solved by assuming the qubit is initially unexcited and the presence of an incident single-photon wavepacket $\varphi_i(x)$, and A is the normalization constant for the two-photon wavepacket (see the main text). With this expression, the problem of computing for $\psi(x > -a, t)$ becomes well-defined and is solved by FDTD [S2].

Our FDTD code is mainly memory bound. For typical cases (such as Fig. 2) we need at least 128 GB of RAM. For the most extreme case that we explored [$\Gamma\tau \approx 25$ in Fig. 3(a), corresponding to $m = k_0 a/\pi = 40$ with $\omega_0 = 10\Gamma$], we use a machine with 450+ GB of RAM in the local cluster. A rule of thumb for estimating the memory usage is to take $16(2N_x + n_x)N_y/1024^3$ (in GB), where n_x is the number of FDTD steps for completing a round trip between the atom and the mirror; all input parameters are explained in detail in [S2]. In the aforementioned most demanding case, both N_x and N_y are about 1.2×10^5 and $n_x \sim 5000$ (such that one resonant wavelength has $n_x/m \sim 100+$ FDTD steps, yielding an accuracy of order 10^{-4}), so the ψ-array alone takes roughly 438 GB. Useful tricks to explore the large τ regime include reducing ω_0/Γ [since $\Gamma\tau = 2m\pi/(\omega_0/\Gamma)$] and reducing n_x/m. For these reasons we set $\omega_0/\Gamma = 20$ for the plots in Fig. 2 and Fig. 3(b) and $\omega_0/\Gamma = 10$ for the plot in Fig. 3(a), where, as previously mentioned, we explored the regime of long delay time. In this way, with the same amount of memory, we were able to complete more FDTD steps at the expense of reduced accuracy (obviously careful checks were necessary). Note that the larger τ the longer the cutoff time t_f needs to be because of the multiple bounces of the photon field before escaping.

Discrete approach

An alternative approach to simulate the two-photon scattering process consists in modeling it as a CCA comprised of a 1D arrangement of $N \gg 1$ identical resonators of frequency ω_c with nearest-neighbour coupling rate J, with one resonator coupled to the qubit with coupling rate g. Hamiltonian (1) of the main text is thus discretized as

$$\hat{H} = \omega_c \sum_{n=1}^{N} \hat{c}_n^\dagger \hat{c}_n - J \sum_{n=1}^{N} (\hat{c}_n^\dagger \hat{c}_{n-1} + \hat{c}_{n-1}^\dagger \hat{c}_n) + \omega_0 \hat{\sigma}^\dagger \hat{\sigma} + g(\hat{c}_{\frac{a}{\ell}}^\dagger \hat{\sigma} + \hat{c}_{\frac{a}{\ell}} \hat{\sigma}^\dagger), \tag{S2}$$

where $\hat{c}_n$ ($\hat{c}_n^\dagger$) annihilates (creates) a photon on the nth cavity mode while $J = v/(2\ell)$ and $g = V/\sqrt{l}$ (here l stands for the longitudinal size of each fictitious cavity). By introducing the momentum operators $\hat{a}_k = \frac{1}{\sqrt{N}} \sum_x e^{ikx} \hat{a}_x$, with $k \in]-\pi, \pi]$ (we are implicitly rescaling the wavevector as $k := kl$), the first two terms of Eq. (S2), which represent the free field Hamiltonian $\hat{H}_f$, can be arranged in the diagonal form $\hat{H}_\mathrm{f} = \sum_k \omega_k \hat{c}_k^\dagger \hat{c}_k$, with the normal frequencies

$$\omega_k = \omega_c - 2J \cos k \tag{S3}$$

forming a band of width $4J$ centered at the bare cavity frequency ω_c. The dispersion law (S3) is approximately linear for $\omega \simeq \omega_c$. Thus, in the weak-coupling regime $\Gamma \ll 4J$ and for $\omega_c = \omega_0$, Hamiltonian (S2) is a reasonable approximation to the physics of the continuous-waveguide Hamiltonian (1) of the main text. The advantage of using this discrete model is that it can be easily handled numerically up to the third-excitation sector of the Hilbert space. In particular, in this work we simulate the time-dependent Schrödinger equation corresponding to Eq. (S2) for $N \sim 800$ ($N \sim 100$) cavities for the two-(three-) excitation subspace and set $\Gamma/(4J) = (g^2/J)/(4J) \leq 0.1$ in order to be consistent with the weak-coupling assumption. In particular we have used $\Gamma/(4J) = 0.075$ for Figs. 3(c) and 5 and $\Gamma/(4J) = 0.062$ for Fig. 4.

It is worth mentioning that, in the present finite-band CCA, even bound states *outside* the band can occur [S3] (in Ref. [S4] it was shown that they can be populated via two-photon scattering). However, the assumption $\omega_0 = \omega_c$ ($k_0 = \pi/2$) ensures that the BIC lies exactly at the center of the band in a way that processes that excite the bound states outside the continuum are energetically forbidden (see [S3]).

Finally, note that the present discrete approach is straightforwardly extended to describe the two-qubit setup in Fig. 5 of the main text. In this case, we place the two emitters far from the CCA edges to avoid unwanted back-reflection from the array's ends within the considered simulation time.

DERIVATION OF EQ. (8)

The BIC state has the structure (see main text)

$$|\phi_b\rangle = \varepsilon_b|e,0\rangle + \int_0^a \mathrm{d}x \, \Big(f_R(x)\hat{a}_R^\dagger(x) + f_L(x)\hat{a}_L^\dagger(x)\Big)\,|g,0\rangle \tag{S4}$$

where

$$|\varepsilon_b|^2 + \int_0^a \mathrm{d}x\,|f_R(x)|^2 + \int_0^a \mathrm{d}x\,|f_L(x)|^2 = 1, \qquad |\varepsilon_b|^2 = \frac{1}{1+\frac{1}{2}\Gamma\tau}\,. \tag{S5}$$

Based on definitions (5) and (6) of the main text, we thus find that in the case of state (7)

$$P_{\mathrm{e}}(\infty) = \int_a^\infty \mathrm{d}x\,|\xi(x,t)|^2|\varepsilon_b|^2\,, \qquad P_{\mathrm{ph}}(\infty) = \int_a^\infty \mathrm{d}x|\xi(x,t)|^2 \sum_{\eta=R,L}\int_0^a \mathrm{d}y\,|f_\eta(y)|^2\,, \tag{S6}$$

where it is understood that time t is large enough that the scattering is complete. Hence, due to the normalization condition in Eqs. (S5),

$$P_{\mathrm{tr}}(\infty) = P_{\mathrm{e}}(\infty) + P_{\mathrm{ph}}(\infty) = \int_a^\infty \mathrm{d}x\,|\xi(x,t)|^2 = P_{\mathrm{BIC}}\ . \tag{S7}$$

Next, combining the last identity in (S5) with the first of Eqs. (S6) yields $\int_a^\infty \mathrm{d}x\,|\xi(x,t)|^2 = P_{\mathrm{e}}(\infty)/|\varepsilon_b|^2 = (1+\frac{1}{2}\Gamma\tau)P_{\mathrm{e}}(\infty)$. Thereby,

$$P_{\mathrm{tr}}(\infty) = P_{\mathrm{BIC}} = (1+\tfrac{1}{2}\Gamma\tau)P_{\mathrm{e}}(\infty)\,, \tag{S8}$$

which completes the proof of Eq. (8) in the main text.

OPTIMAL WIDTH FOR RESONANT TWO-PHOTON WAVEPACKETS

In Fig. 3(a) of the main text, we plot various probabilities against $\Gamma\tau$, each obtained after an optimization over the wavepacket width Δk. In Fig. S1, we plot the optimal Δk, denoted by Δk_{op}, as a function of $\Gamma\tau$. We find that, for delays such that $\Gamma\tau \lesssim 2\pi$, Δk_{op} scales approximately as $\Delta k_{op} \approx \pi/(2v\tau) = \pi/(4a)$. For larger delays, Δk_{op} instead saturates to a non-zero value (presumably in order to maximize the atomic absorption during the scattering transient). For each set value of $\Gamma\tau$, the optimization was carried out by interpolating the P_{e}'s data computed on a discrete Δk-grid (on a log scale) and working out the Δk at which the curve $P_{\mathrm{e}}(\Delta k)$ exhibits a local maximum.

INCREASING THE BIC GENERATION PROBABILITY

Fig. 4 of the main text reports a paradigmatic example showing that $P_{\mathrm{tr}}(\infty)$ can be strongly increased (compared to the standard choice of an exponential pulse) by engineering the wavepacket shape. Here, we describe how the wavepacket in Fig. 4 was derived.

The BIC generation process would be perfect ($P_{\mathrm{BIC}} = 1$) if, in Eq. (7) of the main text, $\beta_{RR}(x,y,t_f) = 0$, meaning that the *incoming* two-photon wavepacket deterministically evolves at the end of scattering into the BIC plus a (normalized) outgoing single-photon wavepacket $\xi_R(x,t)$. The basic idea is to consider the time-reversed version of such ideal process: the system is initially prepared in the dressed BIC $|\phi_b\rangle$ and an incoming single-photon wavepacket $\xi_{\mathrm{op}}(x,t)$ undergoes scattering resulting in a normalized *outgoing* two-photon wavepacket $\beta_{RR,\mathrm{op}}(x,y,t)$ at the end of scattering [S5]. If such a single-photon wavepacket $\xi_{\mathrm{op}}(x,t)$ exists, then sending on the initially unexcited qubit the time-reversed version of $\beta_{RR,\mathrm{op}}(x,y,t)$ will deterministically yield the BIC (plus an outgoing photon).

Based on the above, we considered a right-incoming, Gaussian, single-photon wavepacket of the form

$$\xi_L(x) = \frac{1}{\sqrt[4]{\pi\Delta x^2}}\, e^{-\frac{(x-x_0)^2}{2\Delta x^2} - ik_0(x-x_0)}, \tag{S9}$$

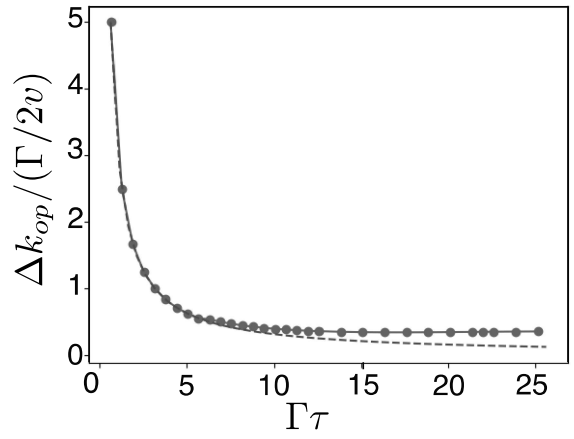

FIG. S1. Optimal wavepacket width Δk_{op} as a function of $\Gamma\tau$, which was used to produce Fig. 3(a) in the main text. The behavior in the range $\Gamma\tau \lesssim 2\pi$ is well fitted by the function $\Delta k_{op} = \pi/(2v\tau)$ (red dashed line). Here we set $\omega_0 = 10\Gamma$.

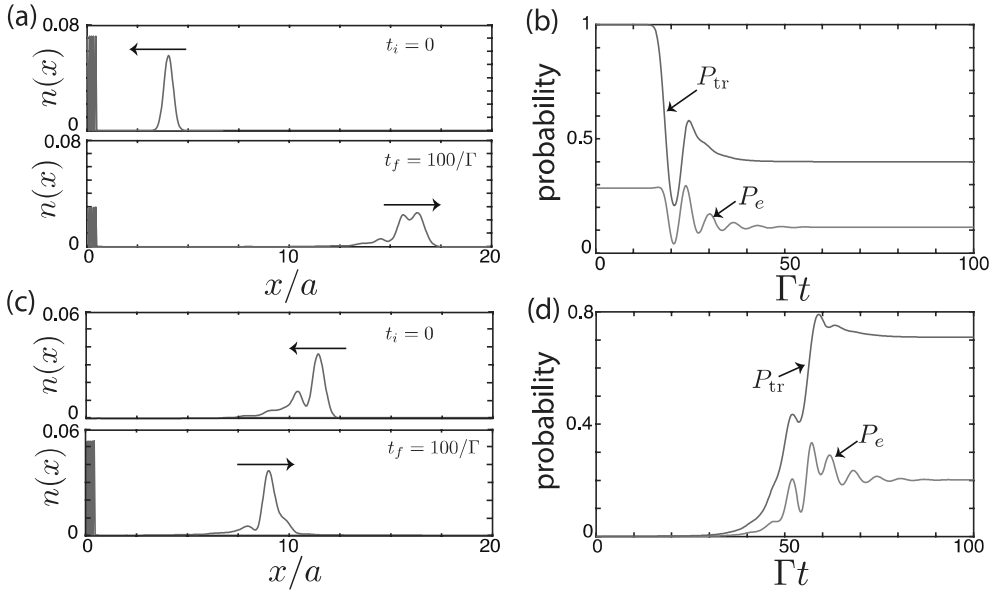

FIG. S2. (a)-(b): Scattering of a single-photon wavepacket with wavefunction (S9) for $\Delta x = 2v/\Gamma$ when the system is prepared in the BIC $|\phi_b\rangle$. (a): Photon-density profile before (top panel) and after (bottom panel) scattering. (b): Time behavior of $P_{\rm tr}$ and $P_{\rm e}$ (see main text) in the same process. (c)-(d): Scattering of the two-photon wavepacket obtained by time-reversing and normalizing the two-photon outgoing component of the previous process. (c): Photon-density profile before and after scattering. (d): Time behavior of $P_{\rm tr}$ and $P_{\rm e}$ in the same process. Throughout, we set $k_0 a{=}20\pi$ and $\Gamma\tau = 5$.

where Δx is the spatial width and $|x_0 - a| > 3\Delta x$, which is injected toward the qubit-mirror region initially prepared in the BIC [see Fig. S2(a)]. At the end of scattering, as shown in Fig. S2(b), part of the excitation trapped in the BIC is released, while a residual amount remains. Minimizing the latter over the width Δx yields $\Delta x = 2v/\Gamma$. The final joint state is of the same form as Eq. (7) in the main text, featuring in particular an outgoing two-photon component. We normalize and time-reverse this two-photon wavefunction, which is then used as the input of our original problem (namely, it is sent to the scattering region with the qubit initially in the ground state) as shown in Fig. S2(c). It turns out [see Fig. S2(d)] that the resulting two-photon-wavepacket is far more effective than the exponential one (see Figs. 2 and 3 in the main text), leading to the BIC generation probability $P_{\rm BIC} = P_{\rm tr}(\infty) \simeq 70\%$.

A further improvement can be obtained by repeating the above process, but this time choosing $\xi_{\rm op}(x,t)$ as the single-photon outgoing component of Fig. S2(c) (once this is normalized and time-reversed). One more iteration of this procedure yields the results in Fig. 5 of the main text, where we obtain in particular $P_{\rm tr}(\infty) \simeq 80\%$ (further

iterations do not substantially change this value).

In this paradigmatic instance, we started from a Gaussian-shaped single-photon wavepacket. Deriving a systematic, general optimization criterion that does not rely on such a specific choice is the target ongoing investigation, in particular with the goal to assess whether the BIC generation probability can approach 100%.

TWO-QUBIT BIC

In Fig. 5(b) of the main text we plot $P_{\rm tr}$, $P_{\rm e}$ and the concurrence C for the two-qubit setup of Fig. 5(a). Here, we provide detailed definitions of these quantities.

As in the case of a qubit in front of a mirror [cf. Eq. (5) in the main text], the joint state at time t lives in the two-excitation sector and thus has the general form

$$|\Psi(t)\rangle = \left(f(t)\hat{\sigma}_1^\dagger\hat{\sigma}_2^\dagger + \sum_{\eta=R,L}\int_{-\infty}^{\infty}\mathrm{d}x\,\psi_{1\eta}(x,t)\hat{a}_\eta^\dagger(x)\hat{\sigma}_1^\dagger + \sum_{\eta=R,L}\int_{-\infty}^{\infty}\mathrm{d}x\,\psi_{2\eta}(x,t)\hat{a}_\eta^\dagger(x)\hat{\sigma}_2^\dagger \right.$$
$$\left. + \sum_{\eta,\eta'=R,L}\frac{1}{\sqrt{2}}\iint_{-\infty}^{\infty}\mathrm{d}x\mathrm{d}y\,\chi_{\eta,\eta'}(x,y,t)\,\hat{a}_\eta^\dagger(x)\hat{a}_{\eta'}^\dagger(y)) \right) |g_1,g_2\rangle|0\rangle\,. \tag{S10}$$

Accordingly, the total probability that at least one qubit is excited reads

$$P_{\rm e}(t) = |f(t)|^2 + \sum_\eta\int_{-\infty}^{\infty}\mathrm{d}x\,|\psi_{1\eta}(x,t)|^2 + \sum_\eta\int_{-\infty}^{\infty}\mathrm{d}x\,|\psi_{2\eta}(x,t)|^2, \tag{S11}$$

while the probability that one photon lies between the two qubits and one beyond them is given by

$$P_{\rm ph}(t) = 2\sum_{\eta,\eta'}\int_{-a}^{a}\mathrm{d}x\int_{-\infty}^{-a}\mathrm{d}y\,|\chi_{\eta,\eta'}(x,y,t)|^2 + 2\sum_{\eta,\eta'}\int_{-a}^{a}\mathrm{d}x\int_{a}^{\infty}\mathrm{d}y\,|\chi_{\eta,\eta'}(x,y,t)|^2\,, \tag{S12}$$

while their sum is called $P_{\rm tr} = P_{\rm e} + P_{\rm ph}$.

To measure the amount of qubit-qubit entanglement in state (S10), we trace out the field degrees of freedom to get the reduced two-qubit density matrix and next calculate the corresponding Wootters concurrence [S6]. This takes the form

$$C(t) = \max\left(0, 2|C_{12}(t)| - \sqrt{|f(t)|^2 P_{\rm ph}}\right), \tag{S13}$$

where

$$C_{12}(t) = \sum_\eta\int_{-\infty}^{\infty}\mathrm{d}x\,\psi_{1\eta}^*(x,t)\psi_{2\eta}(x,t) \tag{S14}$$

are the atomic coherences.

RESILIENCE TO QUBIT LOSSES INTO AN EXTERNAL RESERVOIR

In the main text, we considered ideal setups in which each qubit is perfectly coupled to the waveguide. In practice, the emitters may be also in contact with modes other than the waveguide, which introduces additional decay channels. Assuming a Markovian external reservoir and given our purpose of describing a scattering process, such dissipation can be accounted for by adding to the Hamiltonian Eq. (1) of the main text an effective non-Hermitian term [S7, S8] (we consider the setup of Fig. 1 in the main text):

$$\hat{H} \to \hat{H} - i\frac{\gamma_a}{2}\,\hat{\sigma}^\dagger\hat{\sigma} \tag{S15}$$

where γ_a is the decay rate of the qubit into the external environment.

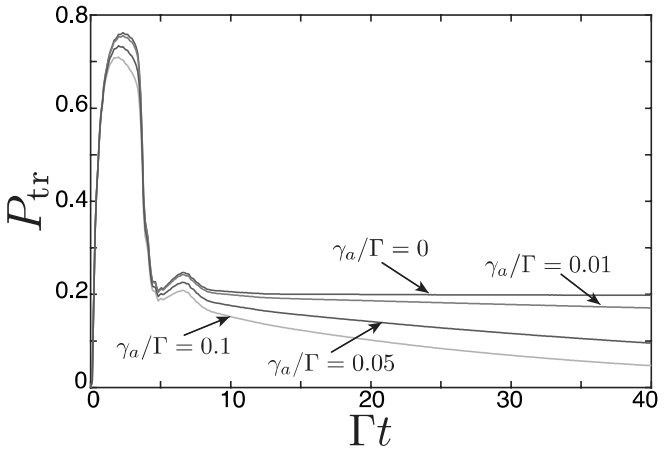

FIG. S3. Trapping probability $P_{\rm tr}$ is plotted against time for different loss rates, γ_a, of the qubit into an external environment for the one-qubit setup of Fig. 1 in the main text. The computation was done using the discrete approach as outlined in Sec. with $\Gamma/(4J) = 0.04$. Other parameters are the same as in Fig. 2.

In Fig. S3, we use the same parameters as in Fig. 2 of the main text and study how the time dependence of $P_{\rm tr}$ is affected by the loss rate γ_a (recall that for $\gamma_a = 0$ the asymptotic value of $P_{\rm tr}$ is the probability of generating the BIC, $P_{\rm BIC}$). In the range considered (γ_a up to 10% of Γ, the decay rate into the waveguide modes) the presence of a nonzero loss indeed turns the long-time saturation at $P_{\rm BIC}$ into a slow decay. We found strong numerical evidence that the long-time behavior of $P_{\rm tr}$ is described by the function $P_{\rm tr}(t \gg \tau) \sim P_{\rm tr}(\infty) e^{-\gamma_a |\varepsilon_b|^2 t}$ with $P_{\rm tr}(\infty) = P_{\rm BIC}$ for $\gamma_a = 0$ [see Eqs. (8), (S7) and (S8)] and $|\varepsilon_b|^2$ being the emitter's population in the BIC [see Eqs. (3) and (4) in the main text]. This finding can be heuristically explained through the following simple argument. The non-Hermitian term in Eq. (S15) can be equivalently expressed as $-i\frac{\gamma_a}{2}|e\,0\rangle\langle e\,0|$, where we set $|e\,0\rangle = |e\rangle|0\rangle$. The effective representation of this in the (one-dimensional) BIC subspace is obtained upon projection as

$$|\phi_b\rangle\langle\phi_b| \left(-i\frac{\gamma_a}{2}|e\,0\rangle\langle e\,0|\right) |\phi_b\rangle\langle\phi_b| = -i\frac{\gamma_a}{2}|\langle e\,0|\phi_b\rangle|^2\,|\phi_b\rangle\langle\phi_b| = -i\frac{\gamma_a}{2}|\varepsilon_b|^2\,|\phi_b\rangle\langle\phi_b|\,, \tag{S16}$$

indicating that for $\gamma_a \neq 0$ the BIC decays at rate $\gamma_a|\varepsilon_b|^2$.

It follows that the smaller the excitonic fraction $|\varepsilon_b|^2$, the more robust is the BIC to emitter losses. Since $|\varepsilon_b|^2$ decreases with τ [cf. Eq. (3) in the main text] it turns out that the longer the delay, the more resilient is the BIC generation scheme to loss. This thus embodies a further significant advantage compared to generation schemes based on spontaneous emission (see discussion in the main text), especially if one aims at an almost pure single-photon trapping.

A detailed discussion of the effect of qubit losses on single-photon BICs, which explicitly takes into account the degrees of freedom of the extra reservoir, is presented in Ref. [S9] (in particular it is shown that the external bath dresses the BIC and scattering states without affecting their orthogonality).

ROLE OF EMITTER NONLINEARITY IN THE BIC GENERATION SCHEME

In the main text, we stressed that the qubit nonlinearity is key to generate the BIC. In this section, we further illustrate this point in terms of a bosonic Hamiltonian that depends in particular on the strength of nonlinearity [S4, S10]. For the sake of argument, we focus again on the one-qubit setup of Fig. 1.

Consider the bosonic Hamiltonian

$$\hat{\mathcal{H}}(U) = \hat{H}_{\sigma\to b} + \hat{H}_I(U) \quad \text{with} \quad \hat{H}_I(U) = \frac{U}{2}\hat{b}^\dagger\hat{b}\,(\hat{b}^\dagger\hat{b} - 1)\,. \tag{S17}$$

Here, $\hat{H}_{\sigma\to b}$ is in the same form as $\hat{H}$ in Eq. (1) of the main text except for the replacement $\hat{\sigma} \to \hat{b}$, where $\hat{b}$ and $\hat{b}^\dagger$ fulfill bosonic commutation relations $[\hat{b}, \hat{b}^\dagger] = 1$ and commute with all the waveguide operators. The *quartic* term $\hat{H}_I(U)$ describes a fictitious, on-site boson-boson repulsion at the emitter's location. When this is absent, i.e. for $U = 0$, Eq. (S17) is equivalent to replacing the qubit with a bosonic mode, which makes the total Hamiltonian fully

bosonic and quadratic. For $U \neq 0$, the effect of $\hat{H}_I(U)$ is to make energetically unfavorable the occupation of emitter's number states $|n\rangle = (\hat{b}^\dagger)^n|\text{vac}\rangle/\sqrt{n!}$ with $n \geq 2$ so that in the limit of infinite U this behaves as an effective qubit and we recover the Hamiltonian Eq. (1):

$$\hat{H} = \lim_{U\to\infty} \hat{\mathcal{H}}(U)\,. \tag{S18}$$

We next discuss the cases $U = 0$ and $U \neq 0$ separately.

$$U = 0$$

In this case, the Hamiltonian is bosonic and quadratic and can thereby be diagonalized straightforwardly in terms of the normal modes. In the single-excitation sector $N = 1$, where $\hat{N} = \hat{b}^\dagger\hat{b} + \sum_{\eta=R,L}\int \mathrm{d}x \hat{a}^\dagger_\eta(x)\hat{a}_\eta(x)$, the eigenstates of (S17) consist of scattering states $\{|\phi_k\rangle\}$ and a bound state $|\phi_b\rangle$ such that $\hat{H}_{\sigma\to b}|\phi_k\rangle = \omega_k|\phi_k\rangle$ and $\hat{H}_{\sigma\to b}|\phi_b\rangle = \omega_0|\phi_b\rangle$, respectively. The corresponding wavefunctions are given by $|\phi_j\rangle = \hat{\alpha}^\dagger_j|\text{vac}\rangle$, where $|\text{vac}\rangle = |g\rangle|0\rangle$ and the normal-mode operators $\{\hat{\alpha}_j\}$ are defined as

$$\hat{\alpha}_j = \varepsilon^*_j\, b + \sum_{\eta=R,L}\int_0^\infty \mathrm{d}x\, f^*_{j,\eta}(x)\, a_\eta(x) \tag{S19}$$

with $j = k, b$. Here, the amplitudes $\{\varepsilon_j\}$ and $\{f_{j,\eta}(x)\}$ are the same as those defining the corresponding single-excitation stationary states of the one-qubit Hamiltonian $\hat{H}$. Regardless of N, normal-mode operators $\{\hat{\alpha}_j\}$ allow one to express the Hamiltonian in the diagonal form

$$\hat{\mathcal{H}}(U=0) = \hat{H}_{\sigma\to b} = \int_0^\infty \mathrm{d}k\, \omega_k\, \hat{\alpha}^\dagger_k\hat{\alpha}_k + \omega_0\hat{\alpha}^\dagger_b\hat{\alpha}_b. \tag{S20}$$

In the two-excitation sector, corresponding to $N = 2$, the eigenstates read

$$|1_k1_{k'}\rangle = \frac{1}{\sqrt{2}}\hat{\alpha}^\dagger_k\hat{\alpha}^\dagger_{k'}|\text{vac}\rangle\,,\quad |1_k1_b\rangle = \hat{\alpha}^\dagger_k\hat{\alpha}^\dagger_b|\text{vac}\rangle\,,\quad |2_b\rangle = \frac{1}{\sqrt{2}}\left(\hat{\alpha}^\dagger_b\right)^2|\text{vac}\rangle\,, \tag{S21}$$

with eigenvalues $\omega_k + \omega_{k'}$, $\omega_k + \omega_0$ and $2\omega_0$, respectively. These are physically interpreted as follows:

- states $|1_k1_{k'}\rangle$ are two-photon scattering states describing two incoming photons that scatter off the emitter and mirror and are eventually fully reflected;
- states $|1_k1_b\rangle$ are semi-bound states: one photon scatters off while another photon is confined between the emitter and mirror dressing the emitter so as to form the single-excitation bound state $|\phi_b\rangle$;
- state $|2_b\rangle$ is a two-photon bound state, featuring in particular two photons fully confined within the mirror-emitter interspace.

Based on these, we see that the scheme for generating the BIC via two-photon scattering becomes fully ineffective when the qubit is replaced by a bosonic mode: injecting two photons with the emitter initially unexcited involves only the stationary states $|1_k1_{k'}\rangle$, which have no overlap with other eigenstates $\{|1_k1_b\rangle\}$ and $|2_b\rangle$. The emitter will typically be excited during the scattering transient, but the two photons will be eventually fully reflected with no light confined in the mirror-emitter interspace. This conclusion holds regardless of the parameters, hence in particular no matter how long the time delay.

$$U \neq 0$$

The last conclusion does not hold any more when the fictitious bosonic repulsive term $\hat{H}_I(U)$ is present [cf. Eq. (S17)]. In the two-excitation sector $N = 2$, this takes the effective form $\hat{H}_I^{(N=2)}(U) = U\,|bb\rangle\langle bb|$ with $|bb\rangle = (\hat{b}^\dagger)^2|\text{vac}\rangle/\sqrt{2!}$. Noting now that in the same subspace all the stationary states [see Eq. (S21)] generally feature a term $\propto |bb\rangle$ we see that the repulsive interaction $\hat{H}_I(U)$ mixes together all the eigenstates of $\hat{H}_{\sigma\to b}$. Most importantly, this means that introducing the nonlinearity has in particular the effects of (i) *connecting* two-photon scattering states $\{|1_k1_{k'}\rangle\}$ to semi-bound ones $\{|1_k1_b\rangle\}$ [see Eq. (S21)] and (ii) *eliminating*, as $U \to \infty$, the two-photon bound state $|2_b\rangle$.

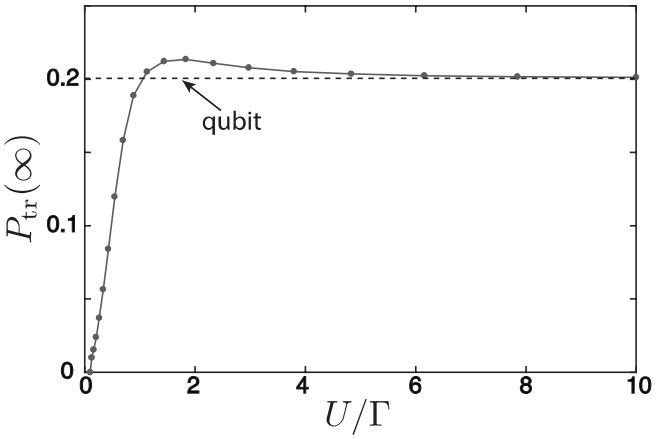

FIG. S4. Asymptotic trapping probability, $P_{\rm tr}(\infty)$, as a function of the nonlinearity parameter U in the case of two photons scattering off a *bosonic* emitter and a mirror (setup analogous to Fig. 1 in the main text) assuming the total Hamiltonian (S17). The black dashed line marks the value of $P_{\rm tr}(\infty)$ when the emitter is a qubit and the total Hamiltonian is the one in Eq. (1) of the main text. The numerical method and parameters are the same as in Fig. S3.

Indeed, using the Lippmann-Schwinger formalism, it can be shown that the $N = 2$ unbound stationary states of $\hat{\mathcal{H}}(U)$ have the following form [S10]

$$|\psi_2(k_1,k_2)\rangle = |1_{k_1}1_{k_2}\rangle + \frac{U\langle bb|1_{k_1}1_{k_2}\rangle}{1-UG_{bb}(E)}\hat{G}^R(E)|bb\rangle, \tag{S22}$$

where $\hat{\mathcal{H}}(U)|\psi_2(k_1,k_2)\rangle = E|\psi_2(k_1,k_2)\rangle$ with $E = \omega_{k_1} + \omega_{k_2}$, $\hat{G}^R(E) = (E - \hat{H}_{\sigma\to b} + i\delta)^{-1}$ is the retarded Green's function for $U = 0$, and $G_{bb}(E) = \langle bb|\hat{G}^R(E)|bb\rangle$. Overlaps between the eigenstate $|\psi_2\rangle$ and other states can be easily computed by noting that all matrix elements can be expressed in terms of the amplitudes $\{\varepsilon_j\}$ and $\{f_{j,\eta}(x)\}$ from the single-excitation sector [S10]. In the limit of $U \to \infty$, Eq. (S22) becomes

$$|\psi_2(k_1,k_2)\rangle = |1_{k_1}1_{k_2}\rangle - \frac{\langle bb|1_{k_1}1_{k_2}\rangle}{G_{bb}(E)}\hat{G}^R(E)|bb\rangle, \tag{S23}$$

which in particular entails $\langle bb|\psi_2\rangle = 0$. Thus, it is clearly impossible to doubly occupy the emitter, and the 2LS behavior is correctly recovered.

This argument provides further physical intuition as to why the nonlinearity of the 2LS, in this picture encoded in the repulsive term $\hat{H}_I(U)$, is essential for the BIC generation scheme via two-photon scattering. In particular, it shows how the intrinsic qubit nonlinearity enables the process where two incoming photons can evolve with some probability into a single scattering photon and the single-photon bound state $|\phi_b\rangle = |1_b\rangle$.

To further support the above conclusion, using the method of Sec. we numerically computed in a paradigmatic case the asymptotic trapping probability $P_{\rm tr}(\infty)$ for the bosonic Hamiltonian (S17) as a function of the nonlinearity parameter U. The definition of $P_{\rm tr}$ is formally analogous to the one where the emitter is a qubit except that the probability of finding the emitter doubly excited (population of state $|bb\rangle$) is now also included. As shown in Fig. S4, $P_{\rm tr}(\infty)$ *vanishes* when $U = 0$ (bosonic emitter) and then overall grows with U, eventually converging as $U \to \infty$ to the corresponding value obtained with a qubit.

As a final remark, we mention that, while for $U = 0$ multi-photon BICs do exist and are simply given by $(\hat{\alpha}_b^\dagger)^n/\sqrt{n!}\,|\text{vac}\rangle$, for the two-level emitter addressed in the main text (corresponding to $U \to \infty$) in the range of parameters considered in this work we did not find any numerical evidence of their existence, which can be checked simply by examining the conservation of probability.

* Present address: ICFO-Institut de Ciencies Fotoniques, 08860 Castelldefels (Barcelona), Spain. Contact email giuseppe.calajo@icfo.eu.
† Present address

[S1] Y.-L. L. Fang, F. Ciccarello, and H. U. Baranger, "Non-Markovian dynamics of a qubit due to single-photon scattering in a waveguide," New J. Phys. **20**, 043035 (2018).

[S2] Y.-L. L. Fang, "FDTD: Solving 1+1D delay PDE in parallel," Comput. Phys. Commun. **235**, 422 – 432 (2019).

[S3] G. Calajó, F. Ciccarello, D. E. Chang, and P. Rabl, "Atom-field dressed states in slow-light waveguide QED," Phys. Rev. A **93**, 033833 (2016).

[S4] P. Longo, P. Schmitteckert, and K. Busch, "Few-photon transport in low-dimensional systems: Interaction-induced radiation trapping," Phys. Rev. Lett. **104**, 023602 (2010).

[S5] M. Cotrufo and A. Alù, "Single-photon embedded eigenstates in coupled cavity-atom systems," (2018), arXiv:1805.03287.

[S6] W. K. Wootters, "Entanglement of formation of an arbitrary state of two qubits," Phys. Rev. Lett. **80**, 2245–2248 (1998).

[S7] J.-T. Shen and S. Fan, "Strongly correlated multiparticle transport in one dimension through a quantum impurity," Phys. Rev. A **76**, 062709 (2007).

[S8] H. Zheng, D. J. Gauthier, and H. U. Baranger, "Waveguide QED: Many-body bound-state effects in coherent and Fock-state scattering from a two-level system," Phys. Rev. A **82**, 063816 (2010).

[S9] C. Gonzalez-Ballestero, F. J. Garcia-Vidal, and E. Moreno, "Non-Markovian effects in waveguide-mediated entanglement," New J. Phys. **15**, 073015 (2013).

[S10] Y.-L. L. Fang and H. U. Baranger, "Waveguide QED: Power spectra and correlations of two photons scattered off multiple distant qubits and a mirror," Phys. Rev. A **91**, 053845 (2015), *ibid.* **96**, 059904(E) (2017).